ELECTRONIC SUPPLEMENTARY MATERIAL

NiTi-Layered Double Hydroxides Nanosheets as Efficient Photocatalysts for Oxygen Evolution from Water using Visible Light

Yufei Zhao,[ac] Bei Li,[a] Qiang Wang,[d] Wa Gao,[a] Chengle J. Wang,[b] Min Wei,*[a] David G. Evans,[a] Xue Duan[a] and Dermot O'Hare*[b]

[a] State Key Laboratory of Chemical Resource Engineering, Beijing University of Chemical Technology, Beijing 100029, P. R. China. Fax: +86-10-64425385; Tel: +86-10-64412131; E-mail address: weimin@mail.buct.edu.cn

[b] Chemistry Research Laboratory, Department of Chemistry, University of Oxford, Mansfield Road, Oxford OX1 3TA, United Kingdom. Tel: +44(0) 1865 272686; E-mail: dermot.ohare@chem.ox.ac.uk

[c] Key Laboratory of Photochemical Conversion and Optoelectronic Materials, Technical Institute of Physics and Chemistry, Chinese Academy of Sciences, Beijing, 100190, P. R. China.

[d] College of Environmental Science and Engineering, Beijing Forestry University, Qinghua East Road, Haidian District, Beijing 100083, P. R. China

TABLE OF CONTENTS

1. Sample Characterization

Powder X-ray diffraction (XRD) patterns of the samples were collected using a Philips PANalytical X'pert Pro diffractometer with Cu-Ka radiation from 8° to 70° with λ= 1.5406 Å, 40 kV, 40 mA. UV–vis spectra were recorded on a Beijing PGENERAL TU-1901 spectrometer in the wavelength range 300–800 nm. The morphology of the layered double hydroxide (LDH) flake was characterized by JEOL JEM-2010 high-resolution transmission electron microscope with an accelerating voltage of 200 kV, and Hitachi H-800 transmission electron microscope (TEM) with an accelerating voltage of 200 kV. AFM (Multimode Nanoscope IIIa, Veeco Instruments) was used to determine the size and thickness of LDH nanosheets. The specific surface area determination was performed by BET methods using a Quantachrome Autosorb-1C-VP analyzer with outgas temperature 120 °C for 6 h. Fluorescence emission spectra were recorded on a RF-5301PC fluorophotometer (1.5 nm resolution) in the range 440–510 nm with the excitation wavelength of 366 nm and slit width of 3 nm. UV–vis spectra were recorded on a Beijing PGENERAL TU-1901 spectrometer in the wavelength range 280–850 nm. X-ray photoelectron spectra (XPS) were recorded using a PHIQ2000 X-ray photoelectron spectrometer equipped with a monochromatic Al K X-ray source. Metallic element analyses were performed by inductively coupled plasma atomic emission spectroscopy (ICP-AES). Carbon, hydrogen, and nitrogen analyses were carried out using a Perkin Elmer Elementarvario elemental analysis instrument. Thermogravimetry and differential thermal analysis (TG-DTA) were carried out on a PCT-1A thermal analysis system under ambient atmosphere with a heating rate of 10 °C$\cdot$min^{-1}. ESR data were recorded on a JES-FA200 Electron Spin Resonance Spectrometer, JEOL. The

Ti K-edge XANES measurements of the samples were performed at the beam line 1W1A at Beijing Synchrotron Radiation Facility (BSRF), Institute of High Energy Physics (IHEP), Chinese Academy of Sciences (CAS) at room temperature in the transmission mode. A CHI 660B electrochemical workstation (Shanghai Chenhua Instrument Co., China) was utilized for electrochemical measurements. A conventional three-electrode cell was used with a saturated Ag/AgCl electrode as the reference, a platinum wire as the counter, and the LDH material modified FTO electrode as the working electrode. The cyclic voltammetry curves were recorded in de-aerated acetonitrile with $LiClO_4$ (0.01 mol/L) as the electrolyte.

2. Photocatalytic Reaction of Splitting Water into Oxygen

The measurement of the photocatalytic O_2 generation activity of the catalysts was carried out as following: 50 mg of the photocatalyst was dispersed in a Pyrex reaction cell using a magnetic stirrer in 50 mL of water, and then 0.01 M $AgNO_3$ was added as a sacrificial reagent. The head space of reactor was sealed with an airtight silicon stopper, and the photocatalyst suspension was thoroughly degassed using argon for 0.5 h. A 300 W Xe lamp (Beijing AuLight Co., Ltd.) was used as a light source. Light was passed through a UV cutoff filter ($\lambda > 400$ nm) and then focused on the reactor. The stationary temperature of the reactor was 38 °C. The formation of oxygen was confirmed by injecting the reactor headspace gas in a gas chromatograph (GC-7890II; Techcomp. Co., Ltd) operating under isothermal conditions (30 °C) equipped with a semicapillary column and a thermal conductivity detector. Photon flux was determined at different wavelength using a monochromator by potassium ferrioxalate actinometry.

3. The Detailed Calculation Information about the Apparent QY

The number of incident photons was calibrated with ferrioxalate solution in the same photo splitting water device. The details are as following:

1) The following procedures should be done under red safe-light. Typically, green crystals of $K_3[Fe(C_2O_4)_3]\cdot 3H_2O$ were prepared by mixing $K_2C_2O_4$ with $FeCl_3$ solution, recrystallized three times from warm water, dried at 45 °C and kept in the dark. Then, a 0.006 M solution was prepared by dissolving the crystals in H_2SO_4 (0.5 M) and diluted with distilled water to 1 L for actinometry. The absorption spectrum of the solution was measured; total absorption at the desired irradiation λ and optical pathlength is recommended.[1]

2) 3 mL (V_1) of the $K_3[Fe(C_2O_4)_3]\cdot 3H_2O$ solution was irradiated under different λ under vigorous stirring. 1 mL (V_2) of the irradiated solution was added into a 10 mL (V_3) volumetric flask containing a mixture of 1,10-phenanthroline solution (store in the dark, 0.1 %, 4 mL) and 0.5 mL of buffer (stock solution: 82 g $NaC_2H_5CO_2$, 10 mL conc. H_2SO_4, diluted to 1 L with distilled water). It is essential that the irradiation time (electronic shutter) as well as the manipulation were controlled very precisely. A reference was prepared in the same way except irradiation. Both solutions are kept in the dark until full color development was achieved, and the absorbance difference between the two samples was measured at 510 nm. The absorbance A (510 nm) should be within the range 0.4–1.8. The photon flux, $q_{n,p}$/einstein s^{-1}, entering the sample cell is given by:

$$q_{n,\mathrm{p}} = \frac{\Delta A \;\; V_1 \;\; V_3}{\Phi(\lambda)\;\; \varepsilon(510\,\mathrm{nm})\;\; V_2 \;\; l \;\; t} \qquad (1)$$

where t is irradiation time. At room temperature, the value of $\Phi(\lambda)$ at different wavelength can be checked according to the reference.[1] In this case, the value of the photon flux must be divided by the fraction of absorbed light at the irradiation wavelength $(1\text{–}10^{-A})$.[2]

4. Computational Details for Band Structure

Plane-wave density functional theory (DFT) calculations for the electron band structure of NiTi-LDH bulk and nano-sized LDH with Ti^{3+} active site were carried out using Dmol3 module in Material Studio 5.5 software package (Accelrys Inc.: San, Diego, CA).[3a] The 3×6×1 supercell (Scheme S1) was adopted for the LDH material as initial structure with lattice parameters $\alpha = \beta = 90°$, $\gamma = 120°$, a = 15.735 Å, b = 6.294 Å, which are in accordance with reported values. The parameter c was referred to the experimental data of this work (7.160 Å for Ni_4Ti-LDH). The generalized gradient approximation (GGA)[3b] with Perdew-Burke-Ernzerhof (PBE)[3c] functional was employed for the DFT exchange correlation energy, and 340 eV of cutoff was assigned to the plane-wave basis set. The self-consistent field (SCF) tolerance was 1×10^{-6} eV. The Brillouin zone was sampled by 1×1×1 k-points. The core electrons were replaced with ultrasoft pseudo-potentials.[3d]

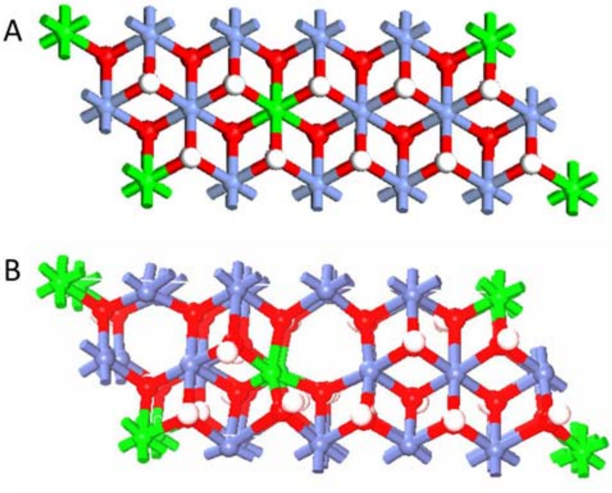

Scheme S1. The supercell model of (A) NiTi-LDH layer with 3×6×1 rhombohedral lattice, (B) NiTi-LDH layer doped with Ti^{3+} defect (Green: Ti; Gray: Ni; Red: O; White: H).

5. Characterizating Data

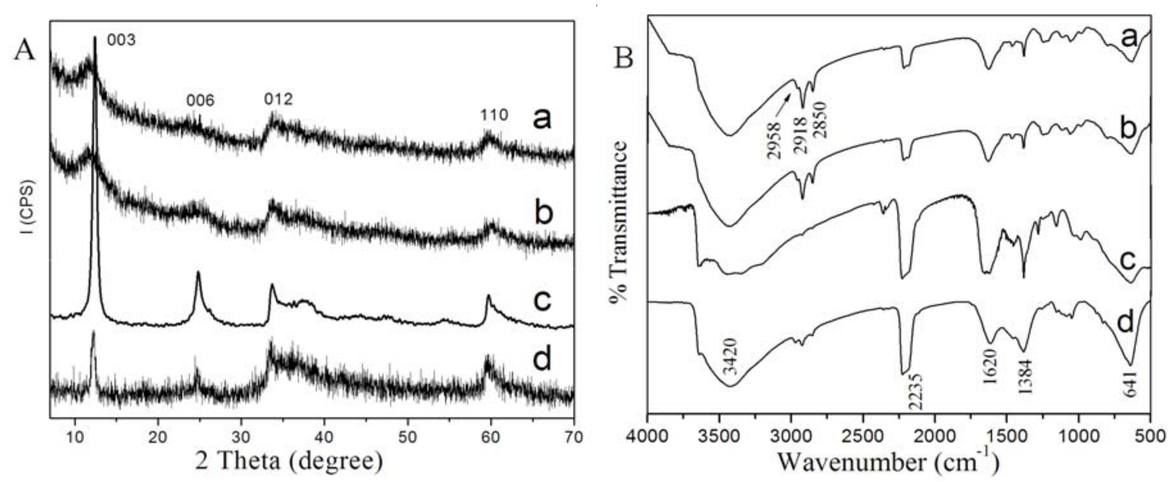

Fig. S1 A. XRD patterns for; (a) NiTi-LDH-1, (b) NiTi-LDH-2, (c) NiTi-LDH-3, (d) NiTi-LDH-4;

B. IR and FT-IR spectra of (a) NiTi-LDH-1, (b) NiTi-LDH-2, (c) NiTi-LDH-3, (d) NiTi-LDH-4.

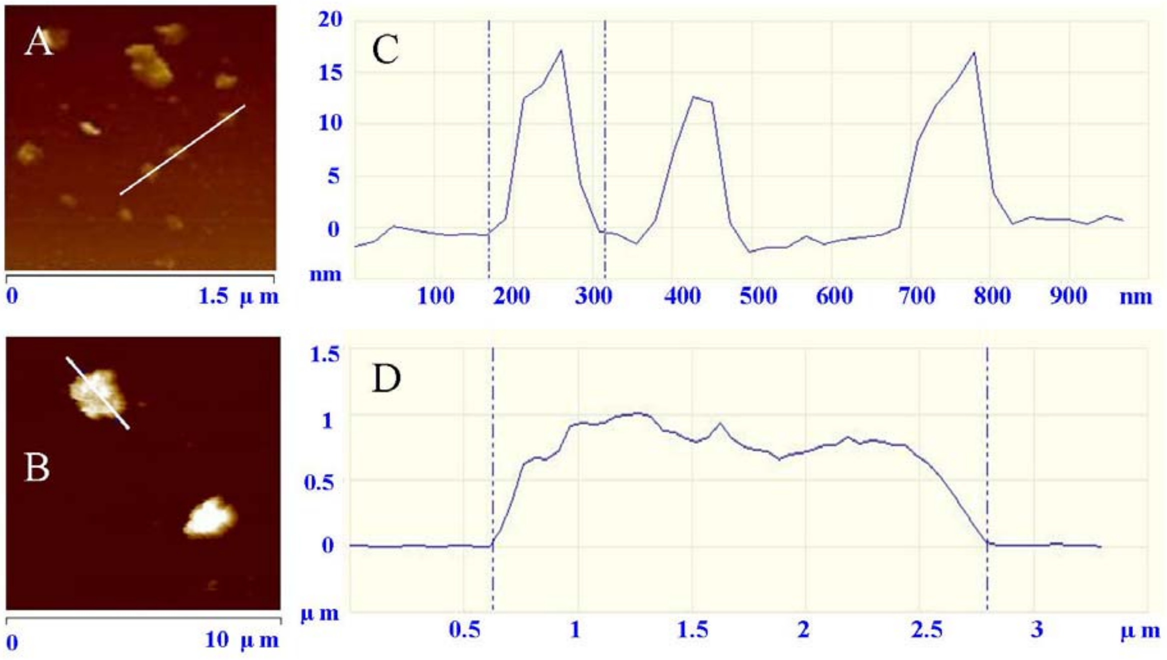

Fig. S2 AFM images of (A) NiTi-LDH-3, (B) NiTi-LDH-4; cross-sectional images of (C) NiTi-LDH-3, (D) NiTi-LDH-4.

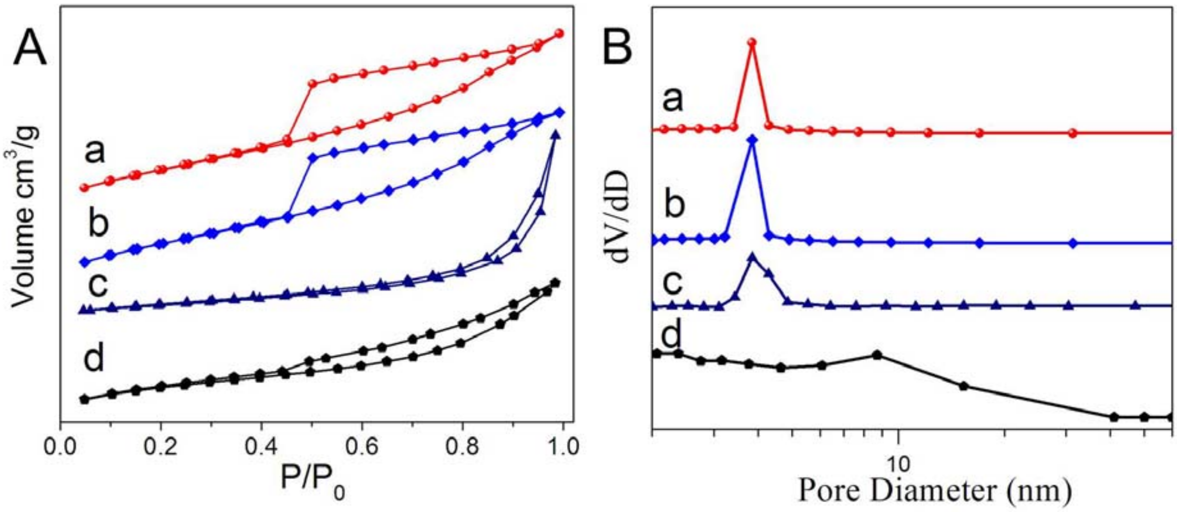

Fig. S3 (A) N_2-sorption isotherms and (B) pore size distribution of (a) NiTi-LDH-1, (b) NiTi-LDH-2 (c) NiTi-LDH-3, (d) NiTi-LDH-4.

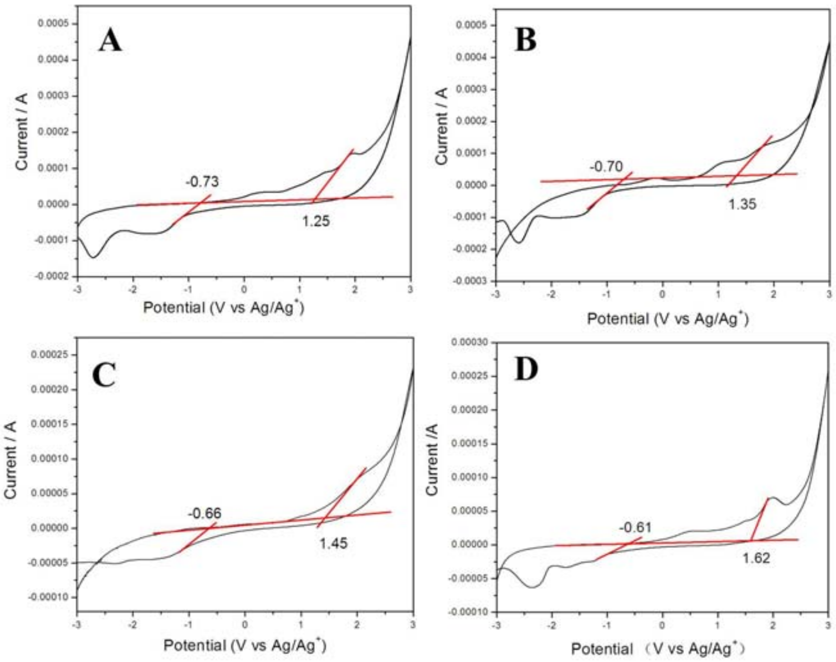

Fig. S4 Cyclic voltammogram curves of (A) NiTi-LDH-1, (B) NiTi-LDH-2, (C) NiTi-LDH-3, (D) NiTi-LDH-4.

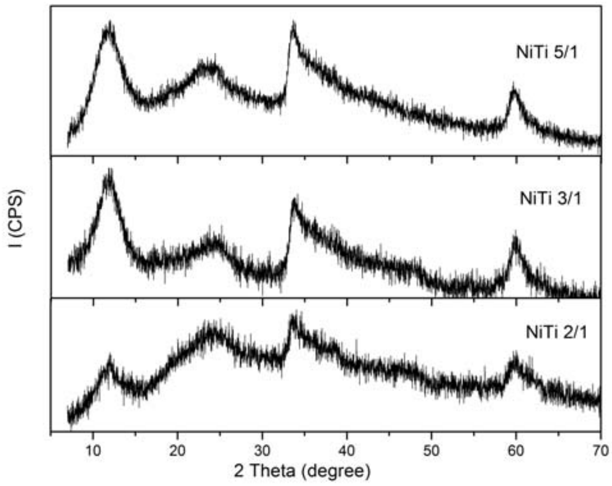

Fig. S5 XRD patterns of NiTi-LDHs with different molar ratio of Ni/Ti.

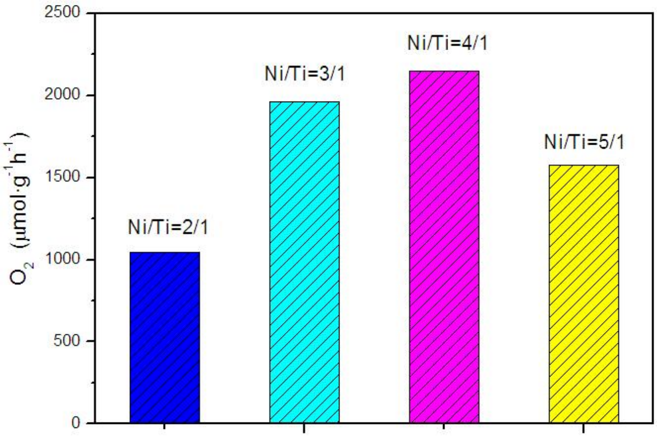

Fig. S6 O_2 evolution in the presence of NiTi-LDH nanosheets with different molar ratio of Ni/Ti.

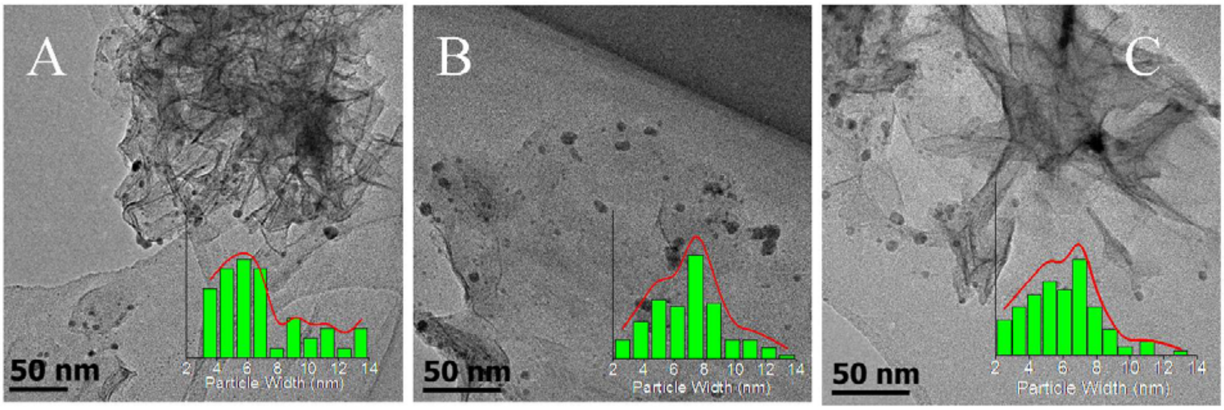

Fig. S7 HRTEM images of the used NiTi-LDH-1 sample after the first (A), second (B) and third cycle (C) of the photocatalytic reaction.

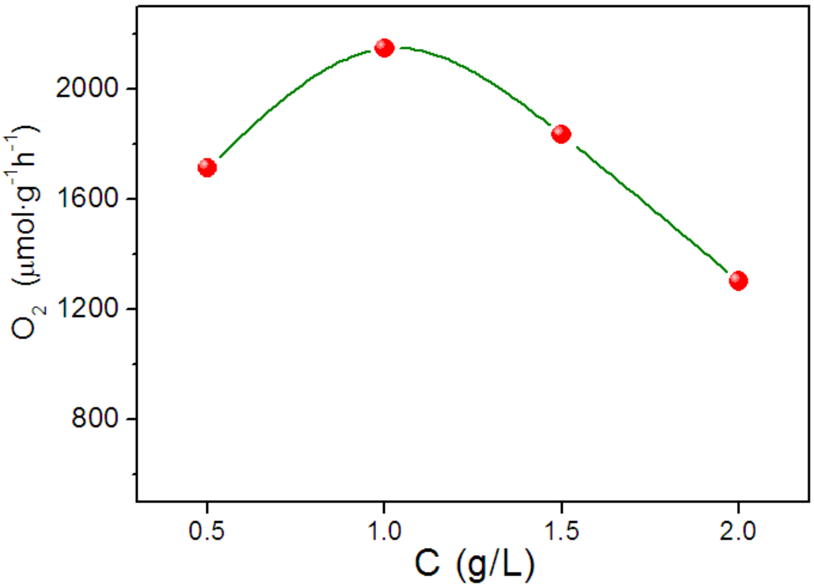

Fig. S8 Initial rate of oxygen production obtained for different NiTi-LDH-1 loadings.

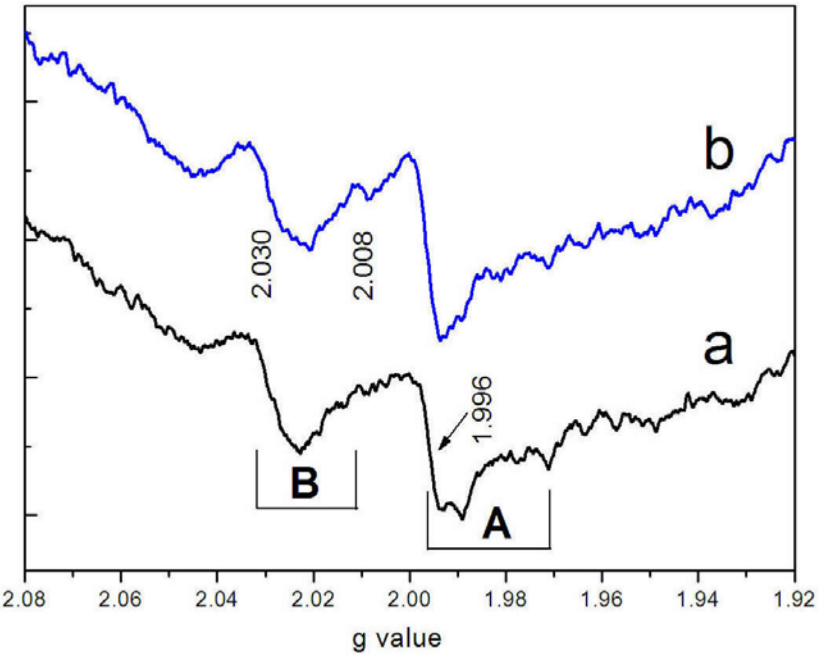

Fig. S9 ESR spectra illustrating the trapped sites at 110 K in vacuum: (a) the fresh NiTi-LDH-1, (b) after 0.5 h of visible-light irradiation.

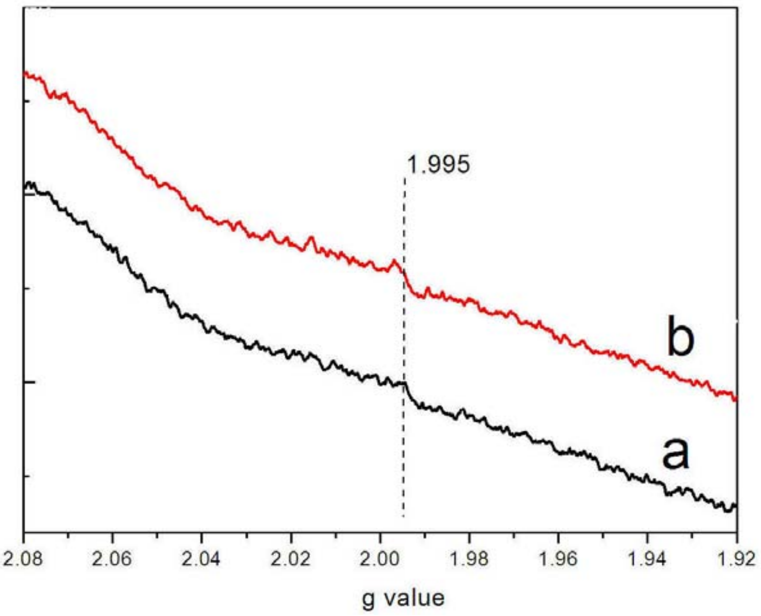

Fig. S10 ESR spectra illustrating the trapped sites at 110 K in vacuum: (a) the fresh NiTi-LDH-4, (b) after 0.5 h of visible-light irradiation.

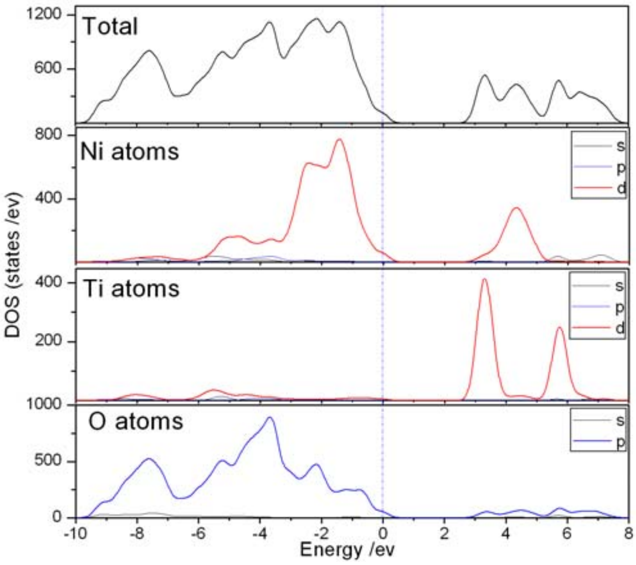

Fig. S11 The total and partial density of states (TDOS and PDOS) of NiTi-LDH-bulk system.[9]

Table S1. Comparison study of visible-light activity of NiTi-LDHs in this work and previously reported photocatalysts towards water splitting to oxygen.

Photo catalyst	**Synthesis method**	**Size (nm)**	**Mass (mg)**	**Surface Area m^2g^{-1}**	**Light**	**Incident light**	**Solution/ Co-catalysts**	**Activity μ mol· $g^{-1}h^{-1}$**	**Activity μ mol· $m^{-2}h^{-1}$**	**QY (%)**	**Refer ence**
TiO_2	Hydro thermal	< 100	200	~ 50	300W Xe	>400 nm	H_2O/ $AgNO_3$	<10	0.2	--	4, 5
ZnCr -LDH	Co-preci-pitation	> 1000	45	67.4[10]	200W Xe	>400 nm	H_2O/ $AgNO_3$	1073	15.9	60.9	6
ZnTi -LDH	Co-preci-pitation	> 1000	45	---	200W Xe	>400 nm	H_2O/ $AgNO_3$	268.3	2.08	--	6
ZnCe -LDH	Co-preci-pitation	> 1000	45	---	200W Xe	>400 nm	H_2O/ $AgNO_3$	626.1	---	--	6
WO_3	Co-preci-pitation	---	45	---	200W Xe	>400 nm	H_2O/ $AgNO_3$	265	---	--	6, 5
NiTi -LDH	Co-preci-pitation	~ 600	200	187.0	300W Xe	700-400 nm	H_2O/ $AgNO_3$	50	0.267	--	4
CuTi -LDH	Co-preci-pitation	---	200	85.0	300W Xe	700-400 nm	H_2O/ $AgNO_3$	30	0.353	--	4
ZnCr/ layered Ti oxide	layer by layer	500-800	10	67.0	450W Xe	>420 nm	H_2O/ $AgNO_3$	1180	17.6	--	7
ZnCr-LDH /RGO	self-assembly	~ 500	10	86.0	---	>420 nm	H_2O/ $AgNO_3$	1200	13.95	61.0	8
NiTi-LDH-1	Reverse micro mulsion	~ 30	50	169.0	300W Xe	>400 nm	H_2O/ $AgNO_3$	2148	12.71	65.0	This work
NiTi-LDH-2	Reverse micro mulsion	~ 60	50	127.4	300W Xe	>400 nm	H_2O/ $AgNO_3$	1714	13.45		This work
NiTi-LDH-3	Co-preci-pitation	~ 90	50	91.4	300W Xe	>400 nm	H_2O/ $AgNO_3$	536	5.86		This work
NiTi-LDH-4	Co-preci-pitation	~ 2000	50	109.4	300 W Xe	>400 nm	H_2O/ $AgNO_3$	267	2.44		This work

Table S2. Chemical composition of NiTi-LDH-*n* samples (*n*=1–4).

Sample	Chemical composition
NiTi-LDH-1	$[Ni_{0.83}Ti^{3+}{}_{0.20}Ti^{4+}{}_{0.02}(OH)_2](CO_3)_{0.12}(CNO)_{0.10}\cdot 0.60H_2O$
NiTi-LDH-2	$[Ni_{0.76}Ti^{3+}{}_{0.08}Ti^{4+}{}_{0.12}(OH)_2](CO_3)_{0.08}(CNO)_{0.08}\cdot 0.60H_2O$
NiTi-LDH-3	$[Ni_{0.82}Ti^{3+}{}_{0.09}Ti^{4+}{}_{0.11}(OH)_2](CO_3)_{0.11}(CNO)_{0.13}\cdot 0.46H_2O$
NiTi-LDH-4	$[Ni_{0.84}Ti^{3+}{}_{0.05}Ti^{4+}{}_{0.13}(OH)_2](CO_3)_{0.17}(CNO)_{0.01}\cdot 0.59H_2O$

References:

1. A. M. Braun, M-T. Maurette and E. Oliveros, *Photochemical Technology*, Wiley, 1991, 70.
2. a) H. J. Kuhn, S. E. Braslavsky and R. Schmidt, *Pure Appl. Chem.*, 2004, **76**, 2105; b) J. Lee and H. H. Seliger, *J. Chem. Phys.*, 1964, **40**, 519.
3. a) M. D. Segall, P. J. D. Lindan, M. J. Probert, J. Pickard, P. J. Hasnip, S. J. Clark and M. C. Payne, *J. Phys. Condens. Matter*, 2002, **14**, 2717; b) J. A. White and D. M. Bird, *Phys. Rev. B*, 1990, **41**, 7892; c) J. P. Perdew, K. Bruke and M. Ernzerhof, *Phys. Rev. Lett.*, 1996, **77**, 3865; d) D. Vanderbit, *Phys. Rev. B*, 1990, **41**, 7892.
4. Y. Lee, J. H. Choi, H. J. Jeon, K. M. Choi, J. W. Lee and J. K. Kang, *Energy Environ. Sci.*, 2011, **4**, 914.
5. X. Chen, S. Shen, L. Guo and Samuel S. Mao, *Chem. Rev.*, 2010**, 110***,* 6503.
6. C. Gomes Silva, Y. Bouizi, V. Fornes and H. Garcia, *J. Am. Chem. Soc.*, 2009**, 131**, 13833.
7. J. L. Gunjakar, T. W. Kim, H. N. Kim, I. Y. Kim and S. J. Hwang, *J. Am. Chem. Soc.*, 2011, **133**, 14998.
8. J. L. Gunjakar, I. Y. Kim, J. M. Lee, N.-S. Lee and S. J. Hwang, *Energy Environ. Sci.*, 2013, **6**, 1008.
9. Y. F. Zhao, P. Chen, B. Zhang, D. S. Su, S. Zhang, L. Tian, J. Lu, Z. Li, X. Cao, B. Wang, M. Wei, D. G. Evans and X. Duan, *Chem. Eur. J.*, 2012, **18**, 11949.
10. L. Tian, Y. F. Zhao, S. He, M. Wei and X. Duan, *Chem. Eng. J.*, 2012, **184**, 261.